

## Error spectrum for the global $M_2$ ocean tide

R. D. Ray,<sup>1</sup> R. J. Eanes,<sup>2</sup> G. D. Egbert,<sup>3</sup> and N. K. Pavlis<sup>4</sup>

**Abstract.** The most accurate determinations of the global ocean tides are currently based on altimeter measurements made by the Topex/Poseidon satellite. The error spectrum corresponding to the  $M_2$  tidal solution is here estimated, primarily by inverse methods and secondarily by simple differencing of several of the best tidal models. The tidal error spectrum is flatter than the tidal signal spectrum, and it exceeds 10% of the signal at spherical harmonic degree 15 and above. The tide errors also exceed the anticipated sensitivity of the upcoming GRACE satellite gravity mission for all degrees below 40, and possibly below 50.

### 1. Introduction

Since the launch of the Topex/Poseidon satellite in 1992 considerable progress has been made in our knowledge of the global ocean tides [e.g., *Le Provost et al.*, 1995]. This progress has been quantified in several ways: by numerous comparisons with *in situ* tide determinations, primarily with coastal tide gauges at small islands and bottom pressure recorders on the sea floor; by variance reduction tests with independent satellite altimeter data; and by comparisons with tidal estimates from satellite tracking [e.g., *Andersen et al.*, 1995; *Shum et al.*, 1997; *Desai et al.*, 1997]. (Tests of tidal current velocities from some of the new tide models have also been made by *Dushaw et al.* [1997] and by others, although tidal currents are not the topic of the present paper.)

Another approach to understanding accuracies of ocean tide models is to determine their error spectra—that is, their error amplitudes as a function of the degree  $n$  of a spherical harmonic expansion. In addition to characterizing model accuracies, reliable error spectra have many applications [e.g., *Tsaoussi and Koblinsky*, 1994]. One application (prompting the present study) involves estimating the effect of aliased tide model errors on monthly determinations of the Earth's gravity field as anticipated to occur during the upcoming GRACE satellite mission. The first step of this work is to determine the error spectrum of the best available models.

The tidal error spectrum is estimated here by two complementary methods: by computing differences in existing models and by estimating errors through global inverse calculations where reasonably realistic *a priori* error covariances are employed. Because we are interested in the effect of tide model errors on the gravity field as determined by satellite geodesy, the error is expressed in terms of equivalent geoid height error, as was recently done by *Wahr et al.* [1998]. Two possible systematic errors in the conversion to tidal geoid variations are also examined: the common assumptions of a constant seawater density and of a spherical earth. In this note we confine ourselves to the dominant semidiurnal lunar tide  $M_2$ .

### 2. Formalism

We employ the spherical harmonic normalization commonly used in physical geodesy [*Heiskanen and Mortiz*, 1967], where the Legendre functions  $P_n^m(\cos\theta)$  satisfy

$$\int_{-1}^1 [P_n^m(\mu)]^2 d\mu = 2(2 - \delta_{m,0}).$$

The contribution of the ocean tides to the geoid undulation  $N$  is expressed as

$$\delta N(\theta, \varphi, t) = a \sum_{n=1}^{\infty} \sum_{m=0}^n P_n^m(\cos\theta) [\delta C_{nm} \cos m\varphi + \delta S_{nm} \sin m\varphi] \quad (1)$$

where  $a$  is the earth's mean radius and  $(\theta, \varphi)$  are spherical polar coordinates. The time-varying Stokes coefficients are computed from the tidal elevation  $\zeta(\theta, \varphi, t)$  by [cf. *Wahr et al.*, 1998]

$$\begin{cases} \delta C_{nm}(t) \\ \delta S_{nm}(t) \end{cases} = \frac{a^2 \rho_w (1 + k'_n)}{M_e (2n + 1)} \iint \zeta P_n^m \begin{cases} \cos m\varphi \\ \sin m\varphi \end{cases} d\Omega \quad (2)$$

where  $\rho_w$  is the mean density of the ocean,  $M_e$  is the mass of the earth, and  $k'_n$  is a loading Love number of degree  $n$  which accounts for the geoid perturbation from ocean tidal loading of the solid earth.

Define the Stokes coefficients  $\delta \bar{C}_{nm}$  and  $\delta \bar{S}_{nm}$  as the root mean squares over a complete tidal cycle  $T$  (12.42 hours) of the time-varying coefficients. Then the tidal contribution to the variance of the geoid, taken over the entire globe, is

$$\frac{1}{4\pi T} \iiint \delta N^2 dt d\Omega = a^2 \sum_{n,m} (\delta \bar{C}_{nm}^2 + \delta \bar{S}_{nm}^2).$$

We take the amplitude spectrum to be the quantity

$$\delta N_{nm} = a \left( \delta \bar{C}_{nm}^2 + \delta \bar{S}_{nm}^2 \right)^{1/2} \quad (3)$$

<sup>1</sup>Laboratory for Terrestrial Physics, NASA Goddard Space Flight Center, Greenbelt, Maryland.

<sup>2</sup>Center for Space Research, University of Texas, Austin, Texas.

<sup>3</sup>College of Oceanic and Atmospheric Sciences, Oregon State University, Corvallis, Oregon.

<sup>4</sup>Raytheon ITSS, Greenbelt, Maryland.

The degree amplitude spectrum is [Wahr *et al.*, 1998]

$$\delta N_n = a \left( \sum_{m=0}^n \delta \bar{C}_{nm}^2 + \delta \bar{S}_{nm}^2 \right)^{1/2}. \quad (4)$$

### 3. Tidal error spectra

Figure 1 shows the spectrum of the ocean tide computed from three recent global models of the  $M_2$  ocean tide. (The figure strictly shows the tide elevation spectrum, not the geoid spectrum; the two are related by the factor preceding the integral in (2).) The three models are all deduced from Topex/Poseidon altimetry using different methods of analysis, including (for TPXO.4) formal data assimilation into a hydrodynamic model. All are improvements to earlier tide models that Shum *et al.* [1997] found were among the most accurate of those available for the entire global ocean. Solution GOT99.2 is described by Ray (1999); CSR4.0 is similar in design but different in some details, including the method used for tidal analysis. Assimilation solution TPXO.4 is an update to that described by Egbert *et al.* [1994] and Egbert [1997]. Both CSR4.0 and GOT99.2 default to a purely hydrodynamic solution [Le Provost *et al.*, 1994] in polar regions above the Topex inclination of  $66^\circ$ , while TPXO.4 extends polewards via its own linearized hydrodynamic model. The three spectra are clearly in close agreement, although careful examination reveals minor differences. The largest variation in the spectra is a function of degree  $n$ , not order  $m$ . The corresponding degree amplitude spectrum is shown as the top curve in Figure 2 (based on TPXO.4).

The degree amplitude spectra of the tide model errors, based on different approaches to estimating the errors in the coefficients  $\delta \bar{C}_{nm}$  and  $\delta \bar{S}_{nm}$ , are shown as the colored curves labeled 1–4 in Figure 2. They stem from two complementary methods.

#### 3.1 Error estimates from inverse methods

The assimilation solution TPXO.4 can be viewed as an optimal interpolation or smoothing of the T/P altimeter data, using a covariance determined by the Laplace tidal equa-

tions (LTE) and prior statistical assumptions about the errors in these equations [Egbert *et al.*, 1994]. Posterior errors can thus be calculated to characterize uncertainty in the estimated fields arising from incomplete altimeter coverage and errors in the data. We use a Monte Carlo approach [Dushaw *et al.*, 1997], which we summarize here. A series of random realizations of the LTE forcing error (which accounts for approximations in the equations, bathymetry errors, and numerical grid truncation) are generated using the prior covariance derived in Egbert *et al.* [1994]. For each realization  $i$  the perturbed LTE are solved numerically to yield synthetic tidal elevations  $\zeta_i$ ,  $i = 1, \dots, N$ . (For the results reported here we use  $N = 20$ .) These elevation fields are each sampled with the spatial and temporal pattern of the altimeter, random data errors (representative of noise and non-tidal oceanography in the T/P data) are added, and the synthetic data are inverted (using the same procedure applied to real T/P data to generate TPXO.4) for estimates  $\hat{\zeta}_i$ . The differences  $\zeta_i - \hat{\zeta}_i$  are representative of errors in the assimilation estimates of tidal elevations. The error fields are found to be largest in the polar seas (beyond the satellite data coverage) and in the shallow seas surrounding Indonesia. The root mean square amplitudes of spherical harmonic coefficients of the  $N$  error fields are used to estimate the tidal error spectrum.

Parameters of the prior covariance can be adjusted so that the amplitude and spatial structure of the random realizations  $\zeta_i$  are grossly consistent (in amplitude and spatial structure) with the T/P data, but it must be admitted that significant uncertainties remain about the “true” prior covariance. We have thus performed calculations for several different (consistent) prior covariances to test the sensitivity of our conclusions to poorly constrained parameters. Curves 1 and 2 in Figure 2 give tidal error amplitude spectra calculated using decorrelation length scales of 300 and 600 km, respectively, for the LTE forcing errors. The two curves are in good agreement for degrees less than 10. For higher degrees the shorter dynamical error decorrelation length scale results (quite sensibly) in somewhat larger errors. But differences between the two cases are not so great; both cross the GRACE sensitivity curve near degree 50.

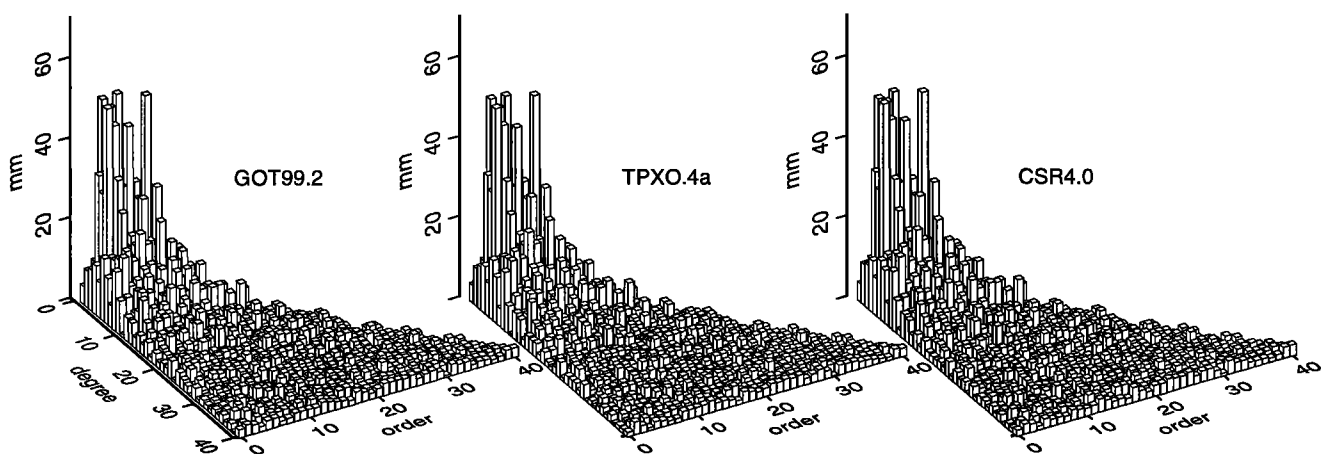


**Figure 1.** Spherical harmonic spectra of three recent global ocean tide models as a function of degree  $n$  and order  $m$ . Vertical axis represents spectral amplitude in sea surface height.

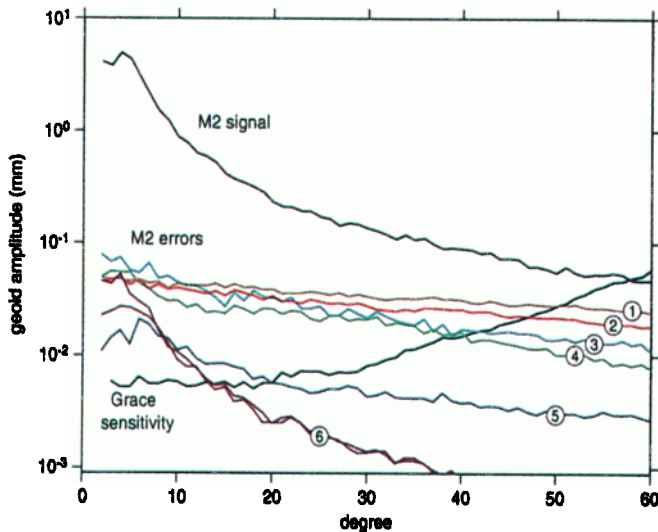


**Figure 2.** Degree amplitude geoid spectra of the global  $M_2$  tide, various estimates of the present-day  $M_2$  errors, and the anticipated sensitivity from 3 months of data from the GRACE satellite gravity mission. Error curves are shown in color and are numbered as follows: (1) inverse estimate corresponding to TPXO.4 assuming a 300-km decorrelation length for the dynamical error covariance; (2) same except with 600-km decorrelation scale; (3) estimate from the difference in models TPXO.4 and CSR4.0; (4) estimate from the difference in models CSR4.0 and CSR3.0; (5) error caused by the neglect of earth flattening; (6) error caused by use of a constant density for seawater, with the larger error employing  $1025 \text{ kg m}^{-3}$  and the smaller the more realistic  $1035 \text{ kg m}^{-3}$ .

### 3.2 Error estimates from model differences

A more simplistic approach to estimating the error in the tidal coefficients is by computing the differences among our three adopted models. Since all are based on the same altimeter data, this approach likely underestimates the errors somewhat, but it is still a useful check on the inverse results.

Figure 3 shows the maximum elevation difference between TPXO.4 and CSR4.0, computed at every point of the global ocean. Throughout most of the open ocean where Topex/Poseidon data are of greatest benefit, the differences between these two models are small, generally less than 2 cm. In coastal regions where the tidal wavelengths are shorter and the tide is less easily mapped by relatively widely spaced satellite observations, model differences are significantly larger. Some of these differences are also in regions of extremely large tidal amplitudes where even a small percentage error can produce large discrepancies. As expected, model differences are also large in polar latitudes outside the satellite limits; results in these regions rely completely on hydrodynamic modeling and (possibly) a sparse set of tide gauge measurements. Figure 3 certainly suggests locations where future modeling efforts should be directed.

Curve 3 in Figure 2 shows the degree amplitude spectrum computed from Figure 3. A similar result is obtained from differences involving the GOT99.2 model. Curve 4 is a spectrum computed from the difference between CSR4.0 and its earlier version CSR3.0. This curve is especially prone to un-

derestimate the real errors since identical methods of analysis were used, and indeed curve 4 falls below curves 1–3 everywhere except for the very lowest degrees where it rises above curves 1 and 2. Except for these very low degrees, curves 3 and 4 are consistently below curves 1 and 2.

### 3.3 Other systematic errors

Curves 5 and 6 in Figure 2 explore the effect of two possible systematic errors in the estimates of the tidal geoid variations. For this purpose, both assume that there is no error at all in the tidal elevations  $\zeta$  (which are taken from model TPXO.4). Curve 5 shows the error caused by the neglect in Eq. (2) of the earth's flattening. Specifically, it is the spectral difference between a harmonic expansion based upon a spherical earth surface (radius 6371 km) and one based on a "serrated" ellipsoidal surface [Jekeli, 1981]. The error is seen to peak around degrees 5 to 7.

Curve 6 (actually comprising two curves) shows the error caused by the common assumption of constant seawater density, which allowed  $\rho_w$  in Eq. (2) to be outside the double integral. The error in such assumption has been computed by including  $\rho_w$  within the spatial integration where it then represents the average density within the water column at any location. This density has been computed from the *Levitus et al.* [1994] climatological densities. The two error curves correspond to assuming  $\rho_w$  is either a constant  $1025 \text{ kg m}^{-3}$  or  $1035 \text{ kg m}^{-3}$ . The latter is more representative of the true global mean seawater density. The former is more representative of surface waters, and it induces the larger errors, actually crossing several of the other curves below degree 6.

## 4. Discussion

Curves 1–3 in Figure 2 represent our best estimates of the error spectrum for present models of the global  $M_2$  ocean

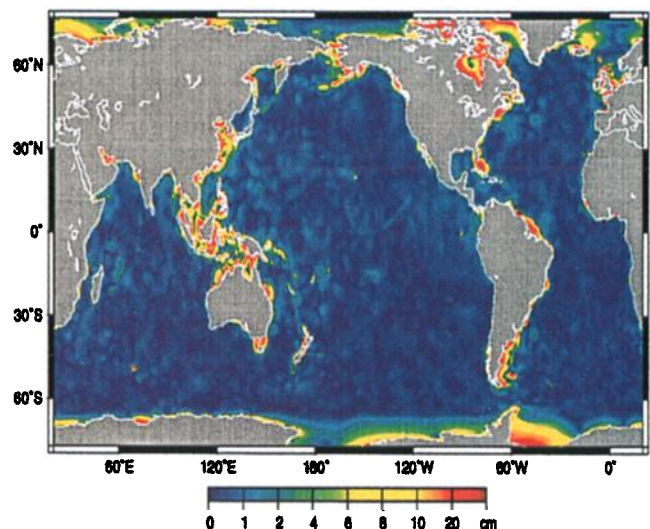


**Figure 3.** Maximum sea surface height difference between the CSR4.0 and TPXO.4 models of the  $M_2$  global ocean tide, in cm. Note the color scale is nonlinear. The maximum difference (in Hudson Strait) exceeds 4 meters. Some basin boundary errors (not in TPXO.4) are discussed by *Smith and Andersen* [1997].

tide. Curve 4 is, as expected, an underestimate. The error spectrum is considerably flatter than the signal spectrum. Above degree 15 or so, the error exceeds 10% of the signal.

Because curve 5 everywhere falls below curves 1–4 we conclude that errors caused by neglecting the earth's flattening are smaller than the errors induced by incomplete knowledge of the tidal elevations  $\zeta$ . Until further significant improvements in  $\zeta$  are forthcoming, the spherical earth approximation appears justified (although the "serrated" ellipsoid approximation is nearly as simple to implement as the spherical approximation). Similarly, errors induced by using a constant seawater density in (2) can be ignored if one adopts a sufficiently representative density near  $1035 \text{ kg m}^{-3}$ ; a density of  $1025 \text{ kg m}^{-3}$  induces errors exceeding curves 1 and 2 when  $n < 5$ .

In the context of the upcoming GRACE gravity field mission, we observe that the expected GRACE sensitivity curve in Figure 2 crosses above the tidal signal curve only at degrees above 56. This implies that ocean-tide force modeling on the satellite must employ much higher degree spherical harmonic expansions than is traditionally done in satellite geodesy.

More importantly, we observe that present-day tide model errors exceed the expected GRACE sensitivity at all spherical harmonic degrees below about 40 or 50. It is important to acknowledge, however, the temporal mismatch in these curves. The GRACE sensitivity corresponds to a long-term (3-month) estimate of the gravity field; the tidal error curves correspond to mean errors over 12.4 hours. To some extent the effect of the tide errors will be mitigated by temporal averaging. To what extent is still unclear. The tide errors will certainly alias into longer, non-tidal periods (depending on the satellite sampling characteristics). Whether the errors could seriously hinder the estimation of the gravity field at the level of the instrument precision or hinder the geophysical interpretation of the gravity field temporal variations is an object of ongoing study.

## References

- Andersen, O. B., P. L. Woodworth, and R. A. Flather, Intercomparison of recent ocean tide models, *J. Geophys. Res.*, *100*, 25261–25282, 1995.
- Desai, S. D., J. M. Wahr, and Y. Chao, Error analysis of empirical ocean tide models estimated from Topex/Poseidon altimetry, *J. Geophys. Res.*, *102*, 25157–25172, 1997.
- Dushaw, B. D., G. D. Egbert, P. F. Worcester, B. D. Cornuelle, B. M. Howe, and K. Metzger, A Topex/Poseidon global tidal model (TPXO.2) and barotropic tidal currents determined from long-range acoustic transmissions, *Prog. Oceanogr.*, *40*, 337–367, 1997.
- Egbert, G. D., Tidal data inversion: interpolation and inference, *Prog. Oceanogr.*, *40*, 53–80, 1997.
- Egbert, G. D., A. F. Bennett, and M. G. G. Foreman, Topex/Poseidon tides estimated using a global inverse method, *J. Geophys. Res.*, *99*, 24821–24852, 1994.
- Heiskanen, W. A. and H. Moritz, *Physical Geodesy*, Freeman and Co., San Francisco, 1967.
- Jekeli, C., The downward continuation to the Earth's surface of truncated spherical and ellipsoidal harmonic series of the gravity and height anomalies, Rep. 323, Dept. Geodetic Science, Ohio State Univ., 1981.
- Le Provost, C., M. L. Genco, F. Lyard, P. Vincent, and P. Canceil, Spectroscopy of the world ocean tides from a finite element hydrodynamic model, *J. Geophys. Res.*, *99*, 24777–24797, 1994.
- Le Provost, C., A. F. Bennett, and D. E. Cartwright, Ocean tides for and from Topex/Poseidon, *Science*, *267*, 639–642, 1995.
- Levitus, S., R. Burgett, and T. Boyer, *World Ocean Atlas 1994*, U. S. Dept. Commerce, Washington, 1994.
- Ray, R. D., A global ocean tide model from Topex/Poseidon altimetry: GOT99.2, NASA Tech. Memo. 209478, 58 pp., 1999.
- Shum, C. K., et al., Accuracy assessments of recent global ocean tide models, *J. Geophys. Res.*, *102*, 25173–25194, 1997.
- Smith, A. J. E. and O. B. Andersen, Errors in recent ocean tide models: possible origin and cause, *Prog. Oceanogr.*, *40*, 325–336, 1997.
- Tsaoussi, L. S. and C. J. Koblinsky, An error covariance model for sea surface topography and velocity derived from Topex/Poseidon altimetry, *J. Geophys. Res.*, *99*, 24669–24683, 1994.
- Wahr, J., M. Molenaar, and F. Bryan, Time variability of the Earth's gravity field: hydrological and oceanic effects and their possible detection using GRACE, *J. Geophys. Res.*, *103*, 30205–30229, 1998.
- R. J. Eanes, CSR, Univ. Texas, 3925 W. Braker Lane, Austin, TX 78759-5321
- G. D. Egbert, COAS, Oregon State University, Corvallis, OR 97331-5503
- N. K. Pavlis, Raytheon ITSS, 7701 Greenbelt Rd., Greenbelt, MD 20770
- R. D. Ray, NASA/GSFC, Code 926, Greenbelt, MD 20771; richard.ray@gsfc.nasa.gov

(Received April 9, 2000; accepted October 4, 2000.)